Supporting Infromation

Selective Detection of Two Representative Organic Arsenics in Aqueous Medium with Metal-Organic Frameworks

Jie Lv,[a] Bin Wang,[a] Yabo Xie,[a] Peilong Wang,*[b] Lun Shu,[a] Xiaoou Su,[b] and Jian-Rong Li*[a]

[a] *Beijing Key Laboratory for Green Catalysis and Separation and Department of Chemistry and Chemical Engineering, College of Environmental and Energy Engineering, Beijing University of Technology, Beijing 100124, P. R. China*

[b] *Institute of Quality Standards and Testing Technology for Agro-products, Chinese Academy of Agricultural Sciences, Beijing, 100081, P. R. China*

To ***Environmental Science: Nano***

Contents

Section 1. Synthesis of H_3CETA

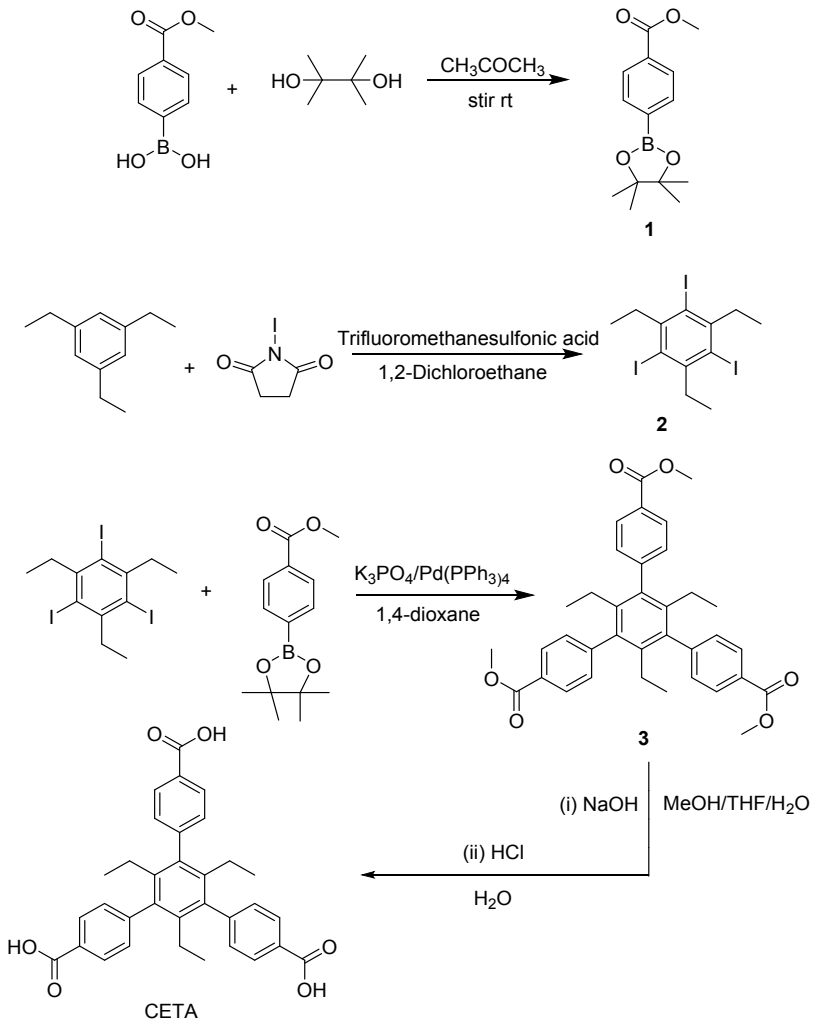

Scheme 1. Synthetic procedure for H_3CETA.

(a) Methyl 4-(4,4,5,5-tetramethyl-1,3,2-dioxaborolan-2-yl)benzoate (1)

To a 1 L three-necked, round-bottomed flask, methyl 4-boronobenzoate (17.0 g, 94 mmol), 2,3-dimethyl-2,3-butanediol (18 g, 152 mmol), and acetone (400 mL) was added. The flask was sealed and stirred at room temperature for 24 hours. The reaction mixture was evaporated on rotary evaporator, and the crude product was chromatographed through silica gel to obtain a white pure solid product (20.0 g, 80%). ^{1}H NMR (400 MHz, $CDCl_3$): δ 8.05 (d, 2H), 7.90 (d, 2H), 3.94 (s, 3H), 1.38 (s,12H).

(b) 1,3,5-Triethyl-2,4,6-triiodobenzene (2)

To a 500 mL three-necked, round-bottomed flask, 1,3,5-triethylbenzene (3.24 g, 20 mmol), N-iodosuccinimide (22.5 g, 100 mmol), 1,2-dichloroethane (120 mL), and trifluoromethanesulfonic acid (60 mg, 0.4 mmol) was added. The flask was equipped with a water condenser and react at reflux for 24 h. After cooling to room temperature, The mixture was diluted with 250 mL of water and filtered to give a crude material. The crude product was washed with water and acetone to give a white solid (8.2 g, 76%). ^{1}H NMR (400 MHz, $CDCl_3$): δ 3.43 (s, 6H), 1.19 (s, 9H).

(c) Dimethyl-2',4',6'-triethyl-5'-(4-(methoxycarbonyl)phenyl)-[1,1':3',1'' -terphenyl]-4,4''-dicarboxylate (3)

To a 1 L three-necked, round-bottomed flask, methyl 4-(4,4,5,5-tetramethyl-1,3,2-dioxaborolan-2-yl)benzoate (13 g, 50 mmol), 1,3,5-triethyl-2,4,6-triiodobenzene (5 g, 9 mmol), K_3PO_4 (15.0 g), and $Pd(PPh_3)_4$ (400 mg) was added. The flask was connected to Schlenk line and evacuated air and refilled with the nitrogen. 300 mL of dioxane and 10 mL of H_2O was degassed (two hours) and added through a canula. The flask was equipped with a water condenser and heated at 95 ^{o}C under the nitrogen for 24 h. The solvent was evaporated on rotary evaporator, and the crude product was filtered and then washed with acetone several times to give the pure product(3.64 g, 70%) ^{1}H NMR (400 MHz, $CDCl_3$): δ 8.12 (d, 6H), 7.41 (d, 6H), 3.96 (s, 9H), 2.04 (s,6H), 0.64 (s, 9H).

(d) 5'-(4-Carboxyphenyl)-2',4',6'-triethyl-[1,1':3',1''-terphenyl]-4,4''-dicarboxylic acid

1 (1.0 g) was suspended in a mixture of THF (90 mL) and MeOH (90 mL), to which 50 mL of 10 M NaOH aqueous solution was added. The mixture was stirred under reflux overnight and the THF and MeOH were removed under vacuum. Dilute HCl was added to the remaining aqueous solution until the solution was at pH = 2. The solid was collected by filtration, washed with water, and dried to give the final product in ~80% yield (0.8 g). ^{1}H NMR (400 MHz, DMSO-d^{6}): δ 8.01 (d, 6H), 7.45 (d, 6H), 1.96 (s,6H), 0.60 (s, 9H).

Section 2. General Characterizations

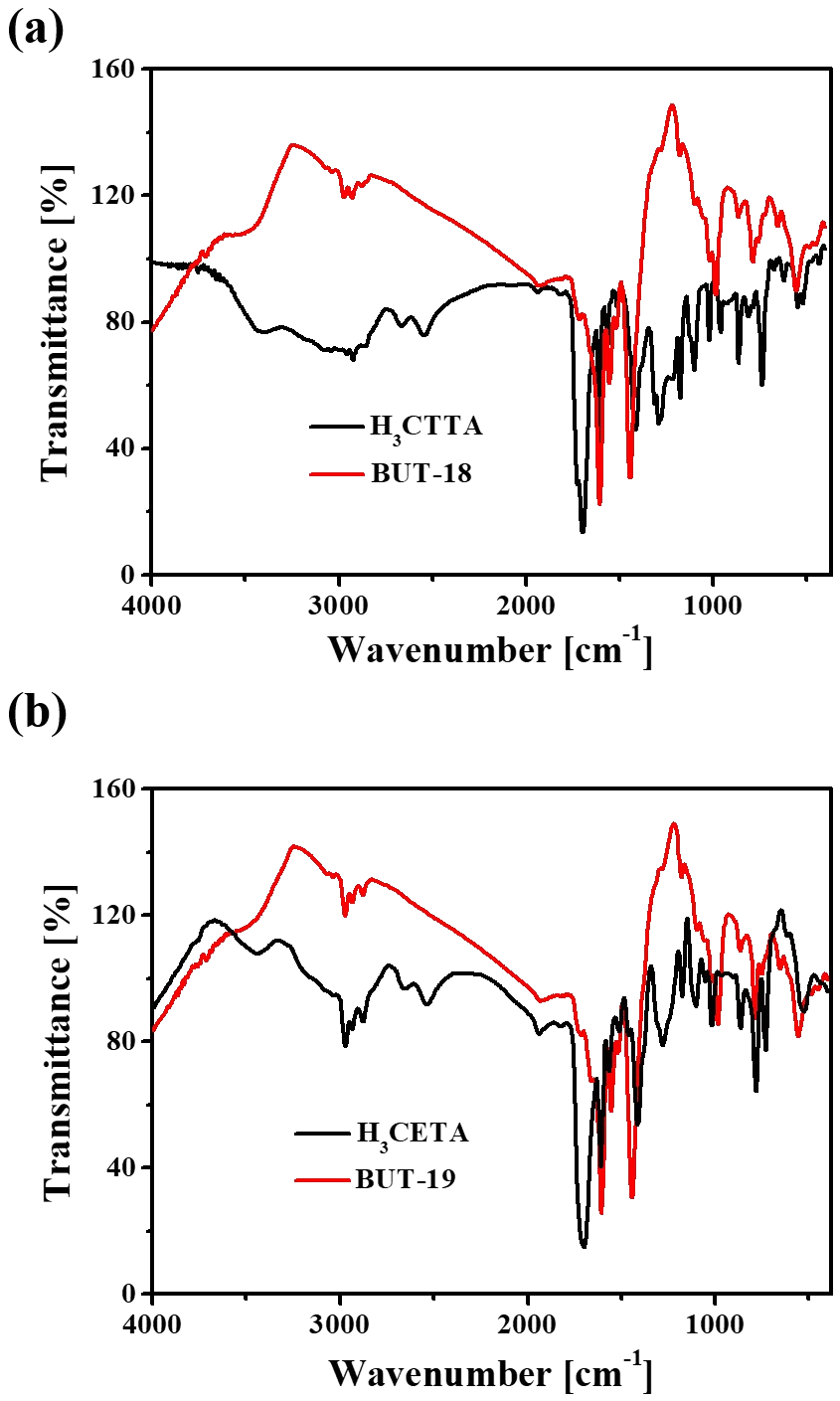

Fig. S1 FT-IR spectra of as-synthesized (a) BUT-18, (b) BUT-19 and their corresponding ligand acids.

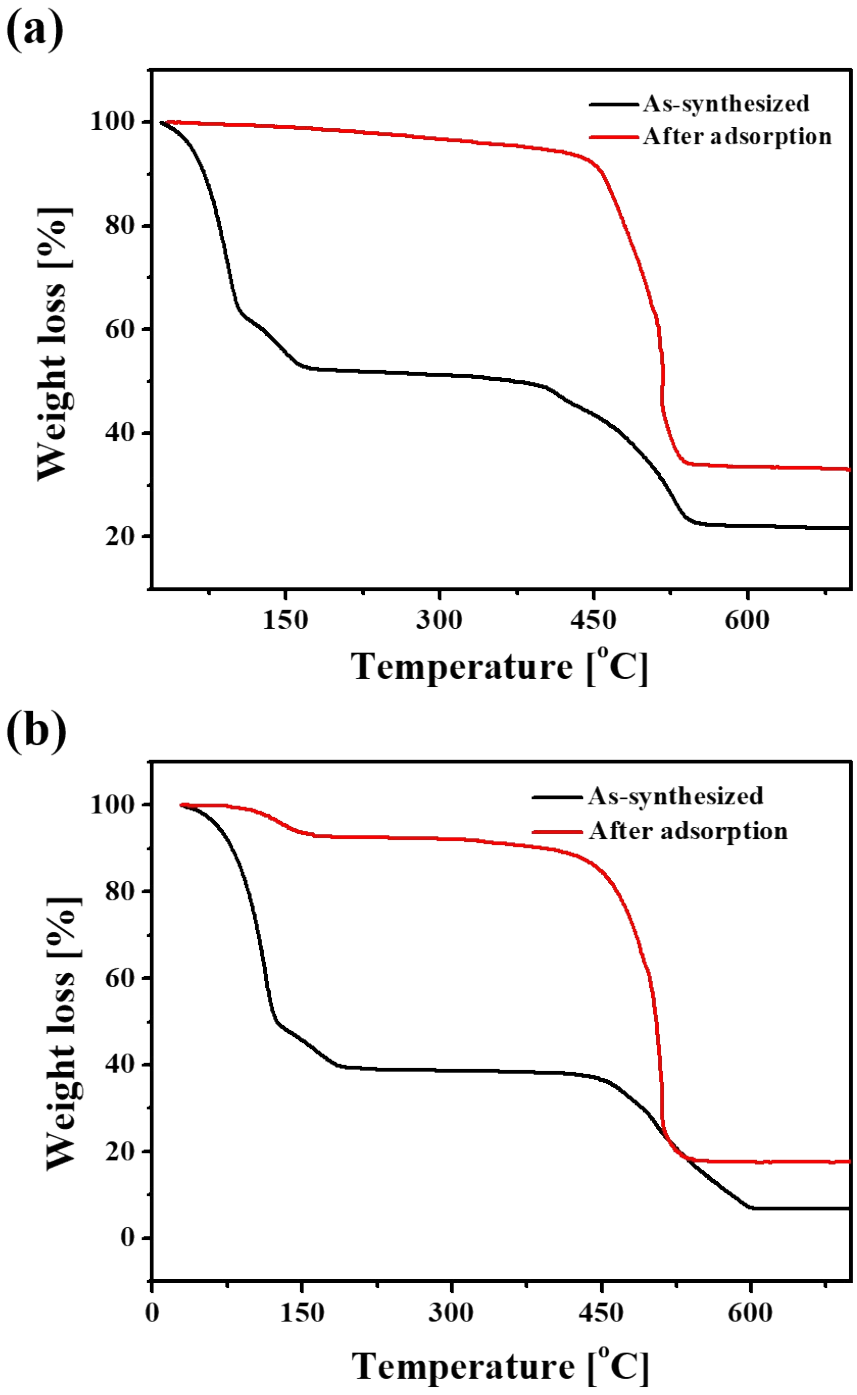

Fig. S2 TGA curves of (a) BUT-18 and (b) BUT-19.

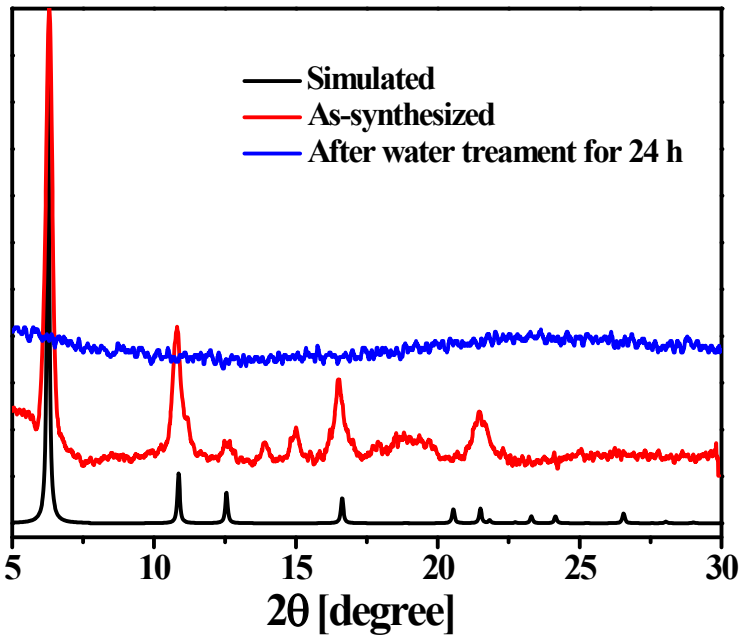

Fig. S3 PXRD patterns of CAU-4.

BET surface area of BUT-18

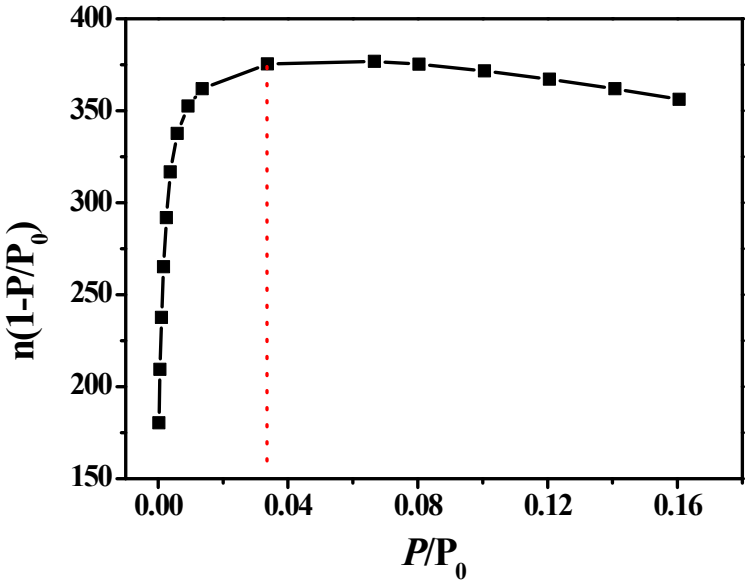

Fig. S4 Plot of n(1-P/P_0) vs. P/P_0 to determine the maximum P/P_0 used in the BET linear fit according to the first BET consistency criterion.

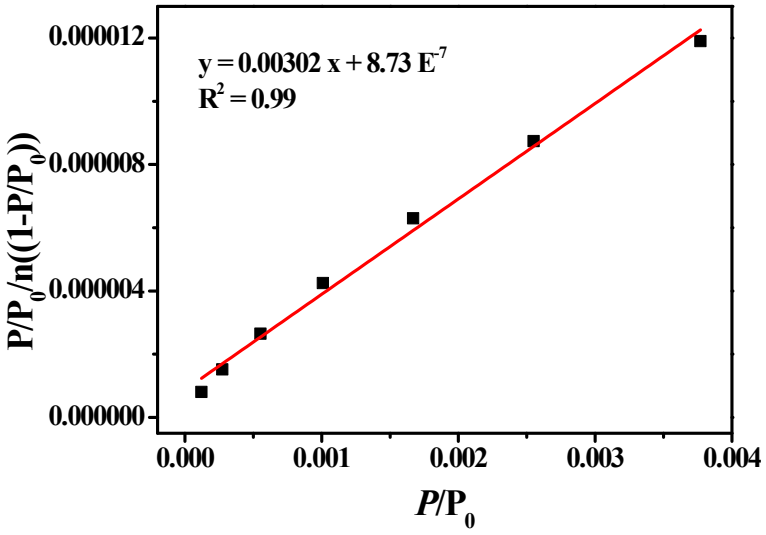

Fig. S5 Plot of $P/P_0/(n(1-P/P_0))$ vs. *P/P0* to determine the BET surface area. The slope of the best fit line for $P/P_0 < 0.004$ is 0.00302, and the y-intercept is 8.73×10^{-7}, which satisfies the second BET consistency criterion. This results in a BET surface area of 1441 $m^2\ g^{-1}$.

BET surface area of BUT-19

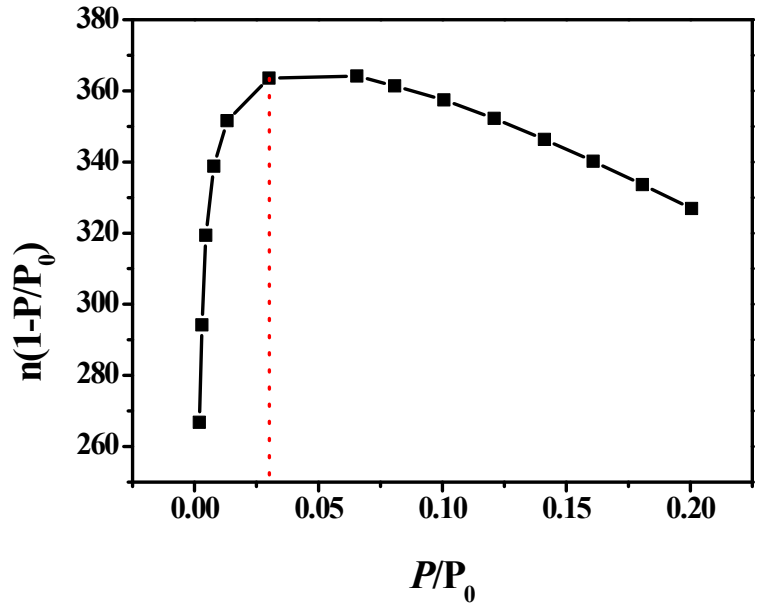

Fig. S6 Plot of $n(1-P/P_0)$ vs. P/P_0 to determine the maximum P/P_0 used in the BET linear fit according to the first BET consistency criterion.

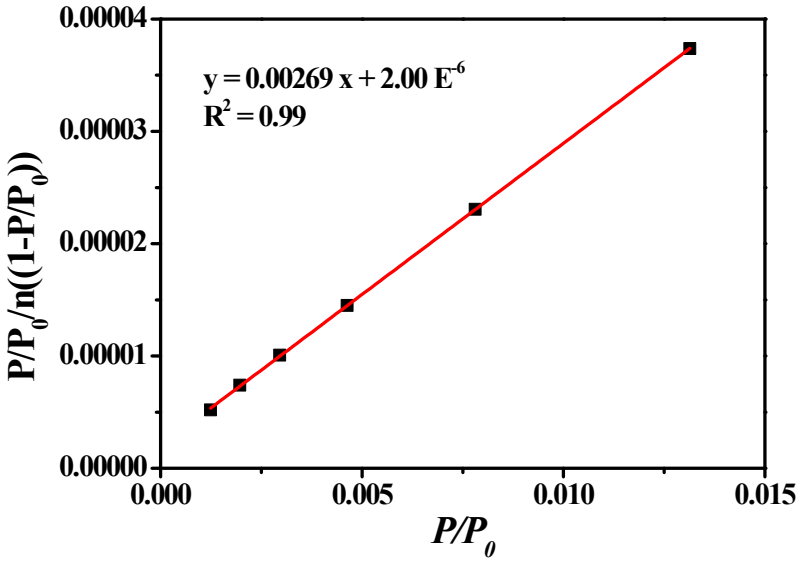

Fig. S7 Plot of $P/P_0/(n(1-P/P_0))$ vs. *P/P0* to determine the BET surface area. The slope of the best fit line for $P/P_0 < 0.015$ is 0.00269, and the y-intercept is 2.00×10^{-6}, which satisfies the second BET consistency criterion. This results in a BET surface area of 1617 $m^2\ g^{-1}$.

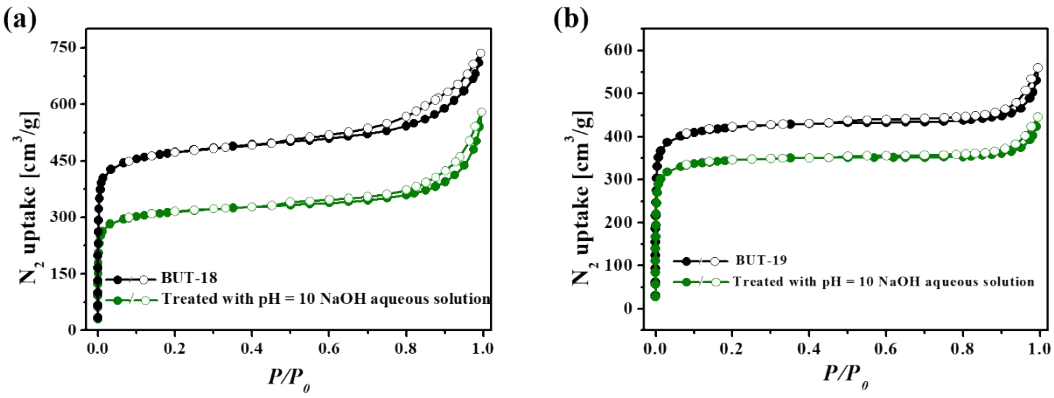

Fig. S8 N_2 adsorption/desorption isotherms at 77 K of (a) BUT-18 and (b) BUT-19 after treated in pH = 10 NaOH aqueous solution for 24 h, respectively.

Section 3. Additional Structural Figure

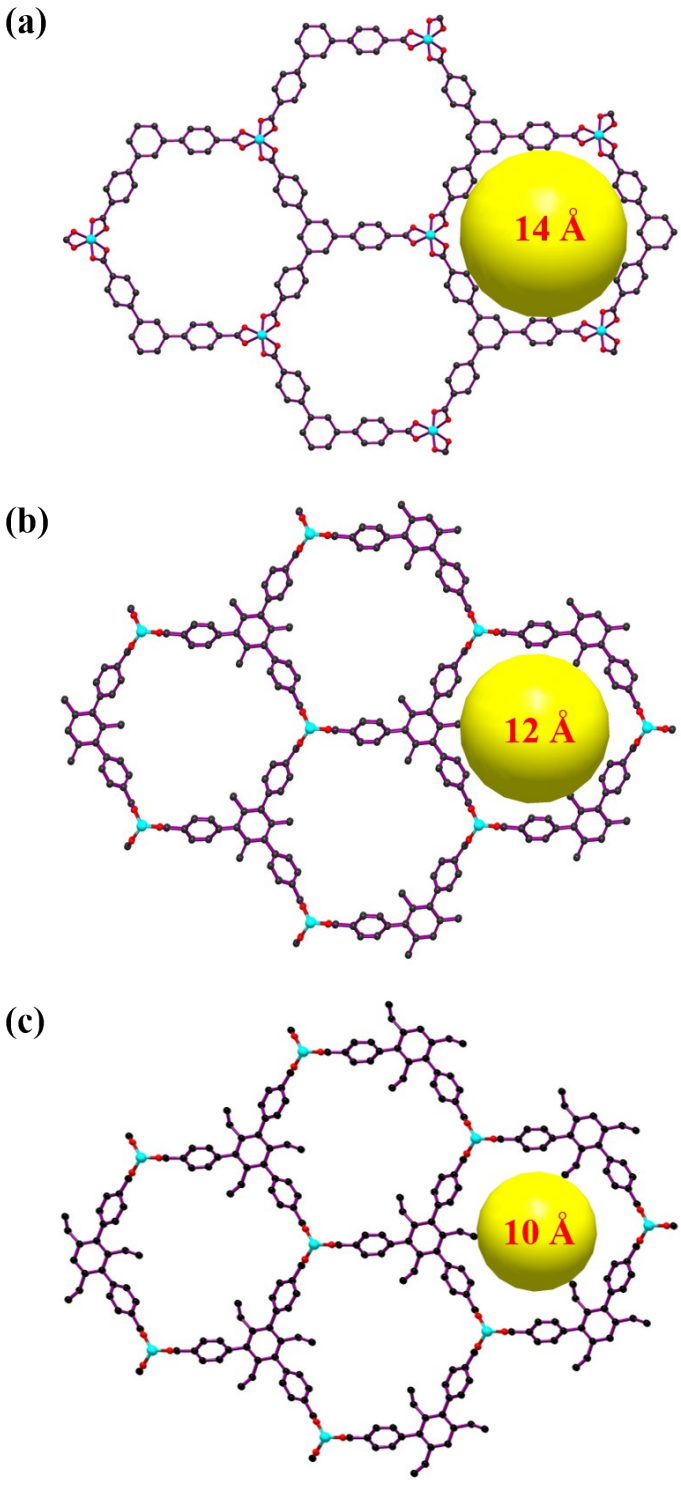

Fig. S9 Three-dimensional framework structure of (a) CAU-4, (b) BUT-18, and (c) with one-dimensional channels along the *c* axis. (H atoms are omitted for clarity, color code: Al, wathet-blue; C, black; O, red).

Section 4. Organic Arsenics detection

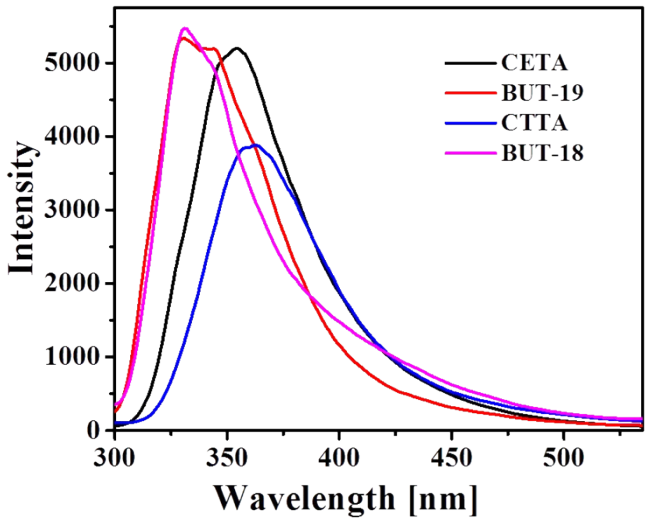

Fig. S10 Solid-state photoluminescent spectra of BUT-18, BUT-19, free H_3CTTA, and free H_3CETA ligand acid excited at 280 nm at RT.

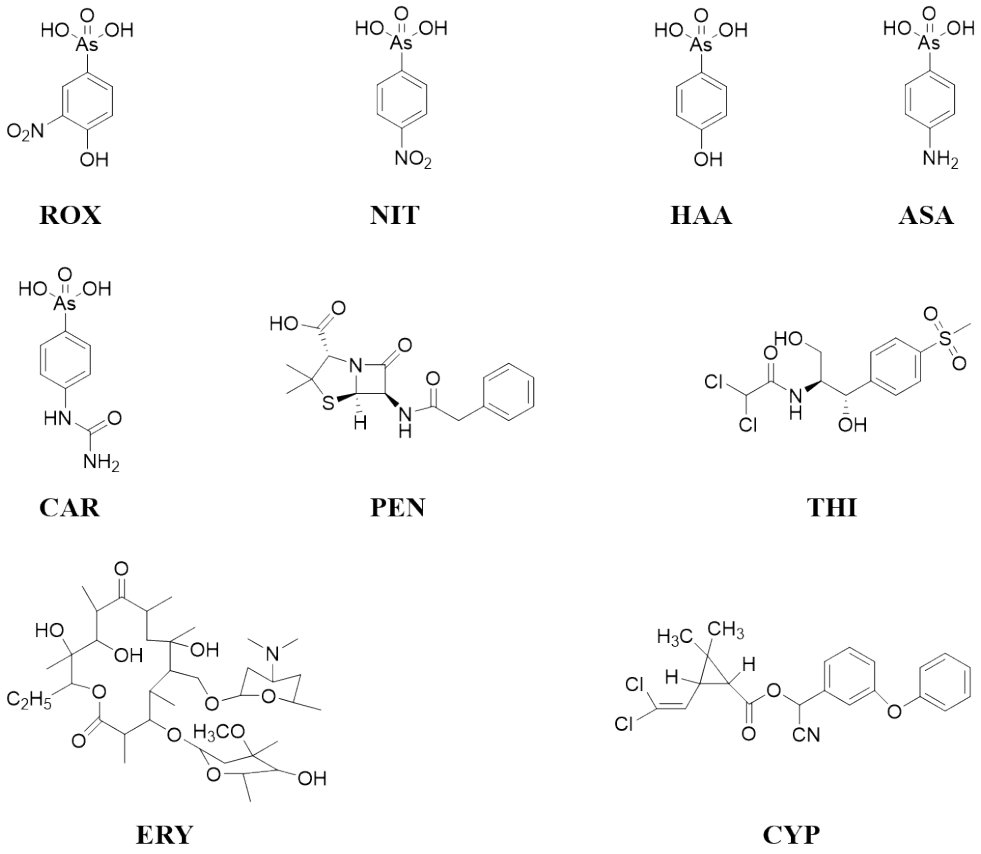

Fig. S11 Chemical structures of selected analytes.

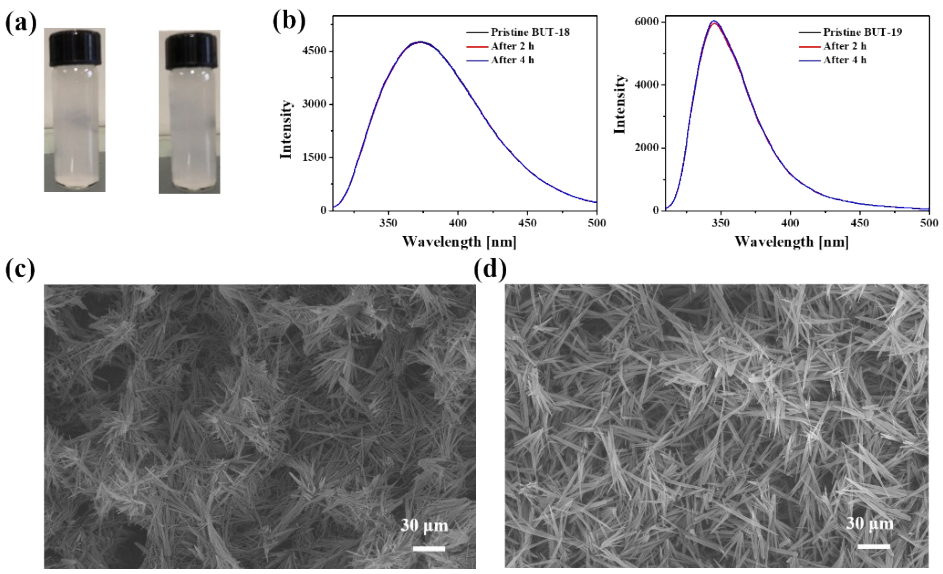

Fig. S12 (a) Photographs of BUT-18 and -19 solutions after 4 hours; (b) fluorescence of BUT-18 and -19 solutions at different times; SEM images of (c) BUT-18 and (d) BUT-19 solution.

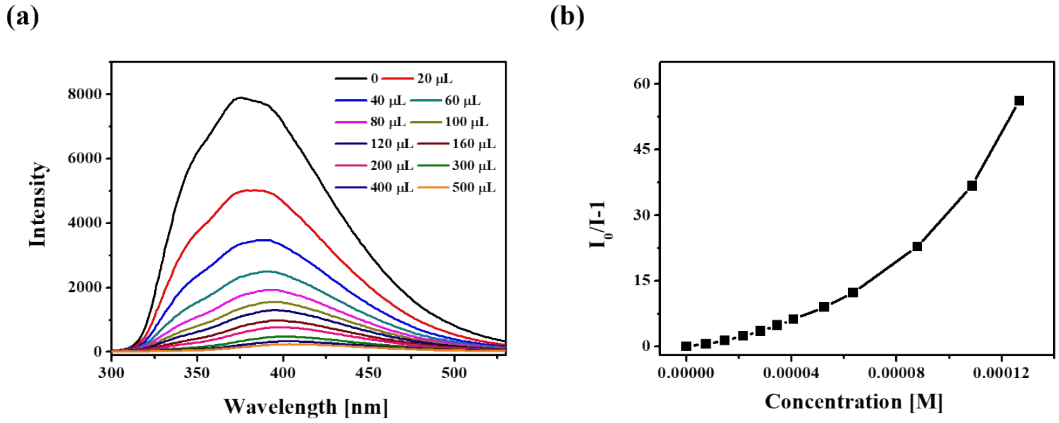

Fig. S13 (a) Effect on the emission spectra of BUT-18 dispersed in water upon the incremental addition of 500 µL (100 ppm) water solution of ROX, (b) Stern-Volmer plot of ROX.

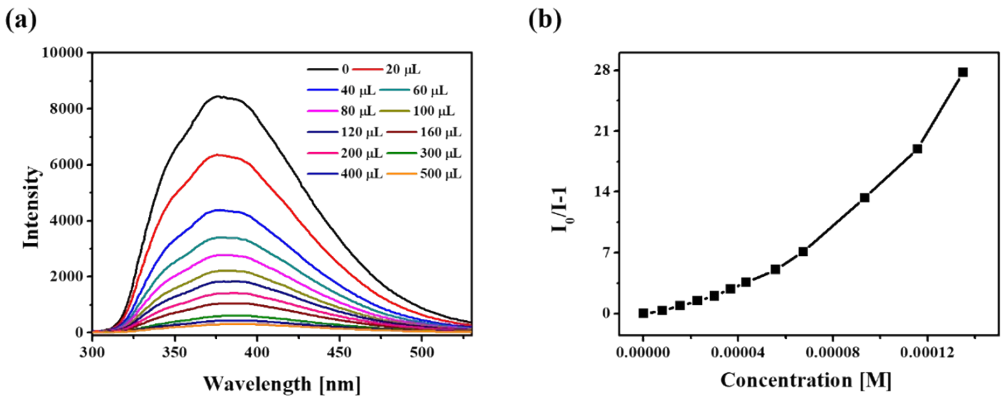

Fig. S14 (a) Effect on the emission spectra of BUT-18 dispersed in water upon the incremental addition of 500 µL (100 ppm) water solution of NIT, (b) Stern-Volmer plot of NIT.

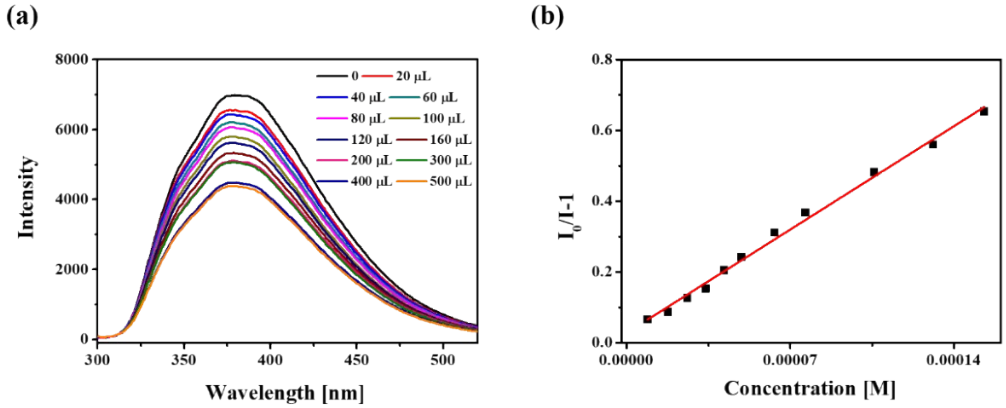

Fig. S15 (a) Effect on the emission spectra of BUT-18 dispersed in water upon the incremental addition of 500 µL (100 ppm) water solution of HAA, (b) Stern-Volmer plot of HAA.

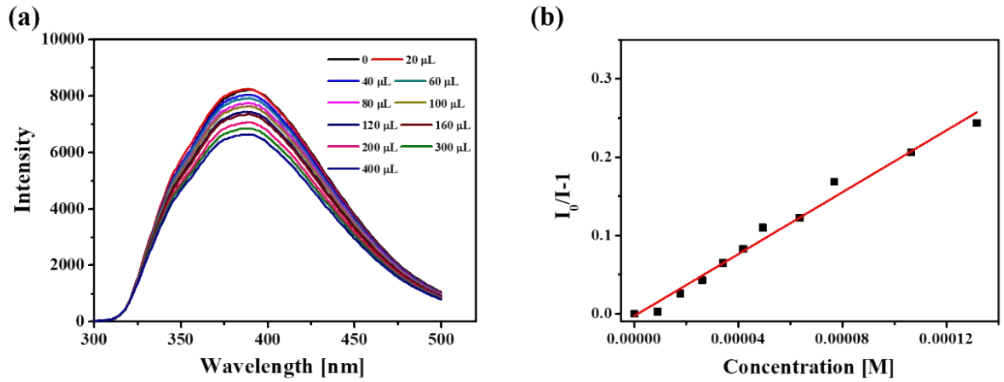

Fig. S16 (a) Effect on the emission spectra of BUT-18 dispersed in water upon the incremental addition of 500 µL (100 ppm) water solution of ASA, (b) Stern-Volmer plot of ASA.

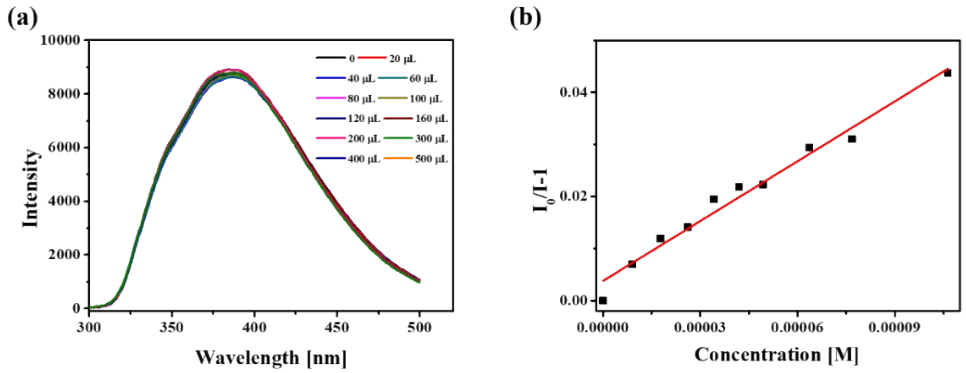

Fig. S17 Effect on the emission spectra of BUT-18 dispersed in water upon the incremental addition of 500 µL (100 ppm) water solution of CAR (inset: Stern-Volmer plot of CAR).

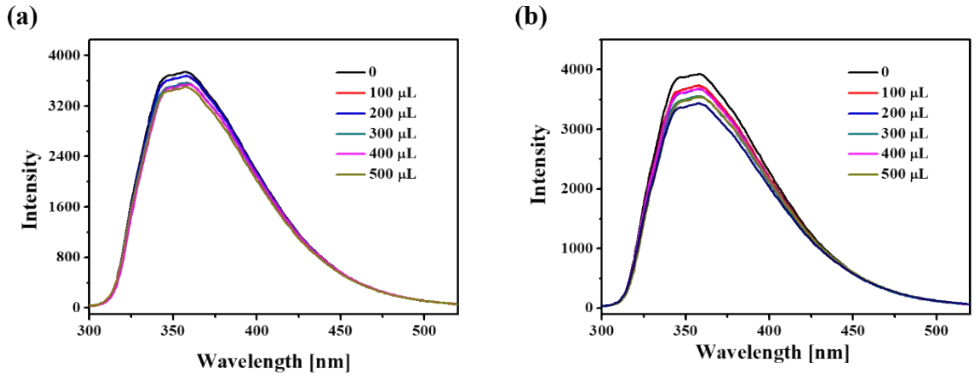

Fig. S18 Effect on the emission spectra of BUT-18 dispersed in water upon the incremental addition of 500 µL (100 ppm) water solution of (a) ERY and (b) THI, respectively.

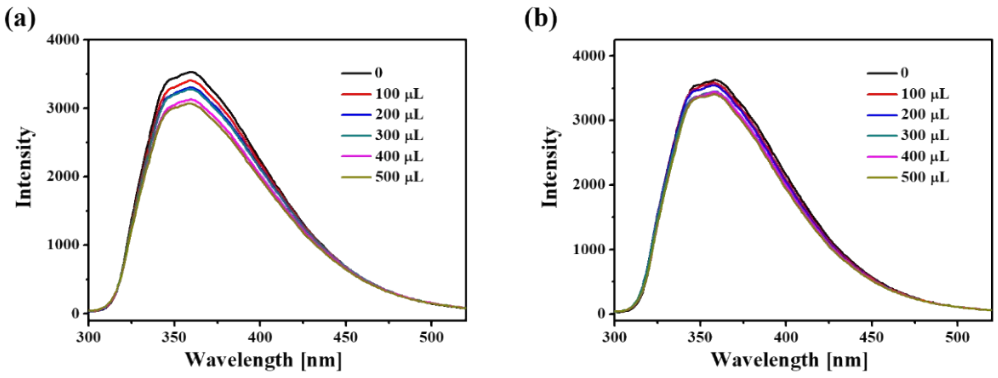

Fig. S19 Effect on the emission spectra of BUT-18 dispersed in water upon the incremental addition of 500 µL (100 ppm) water solution of (a) CYP and (b) PEN, respectively.

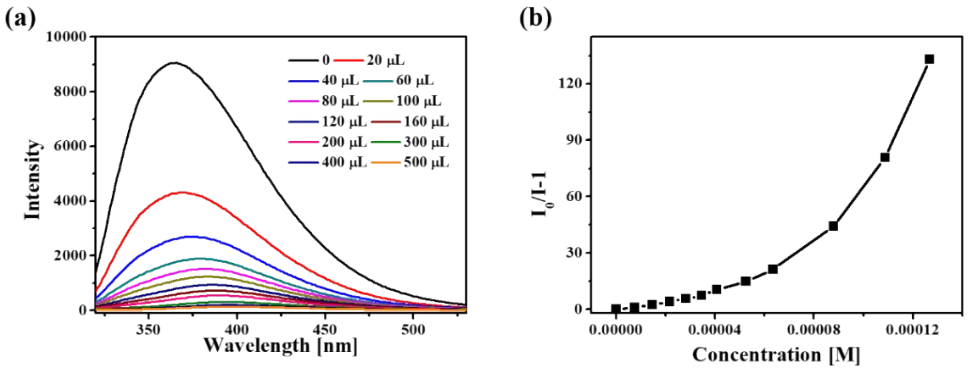

Fig. S20 (a) Effect on the emission spectra of BUT-19 dispersed in water upon the incremental addition of 500 µL (100 ppm) water solution of ROX, (b) Stern-Volmer plot of ROX.

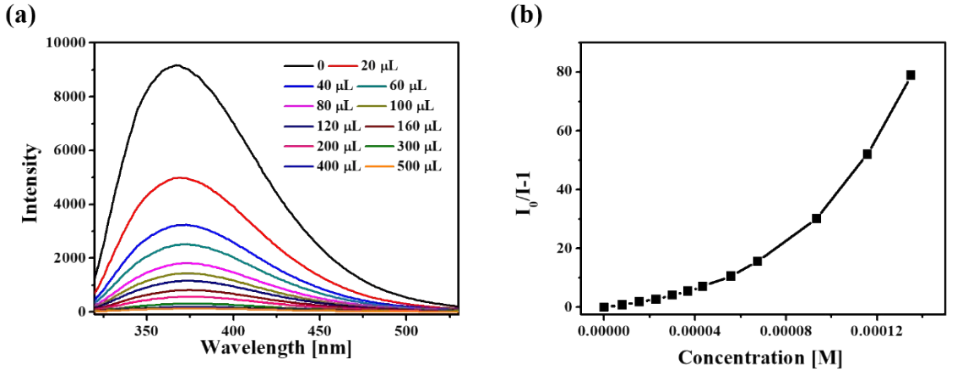

Fig. S21 (a) Effect on the emission spectra of BUT-19 dispersed in water upon the incremental addition of 500 µL (100 ppm) water solution of NIT, (b) Stern-Volmer plot of NIT.

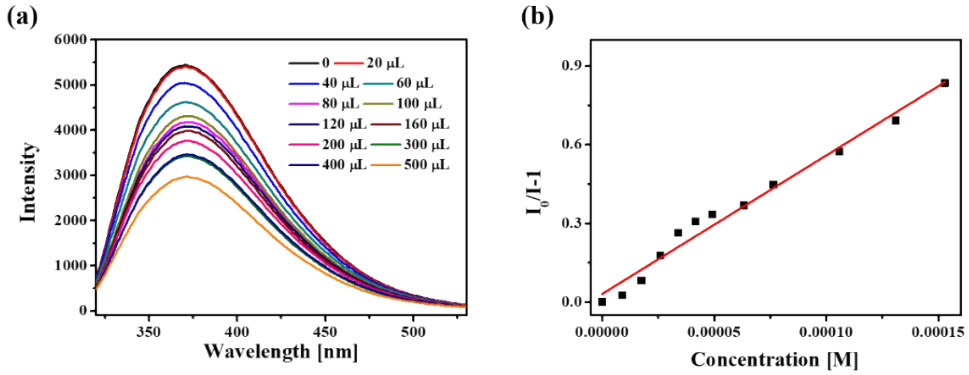

Fig. S22 (a) Effect on the emission spectra of BUT-19 dispersed in water upon the incremental addition of 500 µL (100 ppm) water solution of HAA, (b) Stern-Volmer plot of HAA.

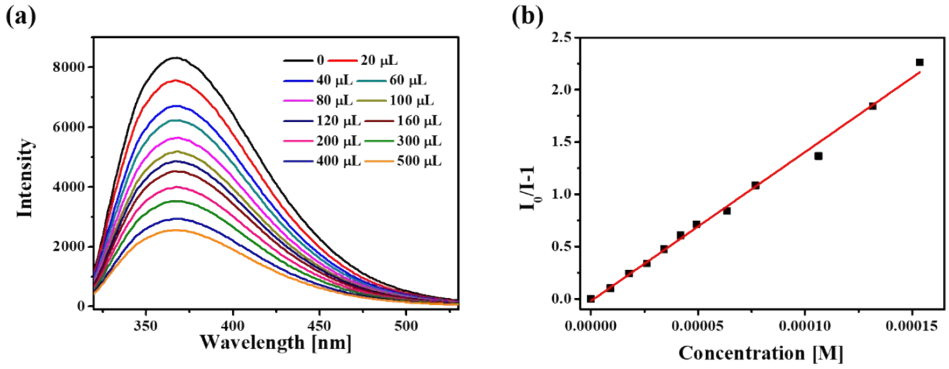

Fig. S23 (a) Effect on the emission spectra of BUT-19 dispersed in water upon the incremental addition of 500 µL (100 ppm) water solution of ASA, (b) Stern-Volmer plot of ASA.

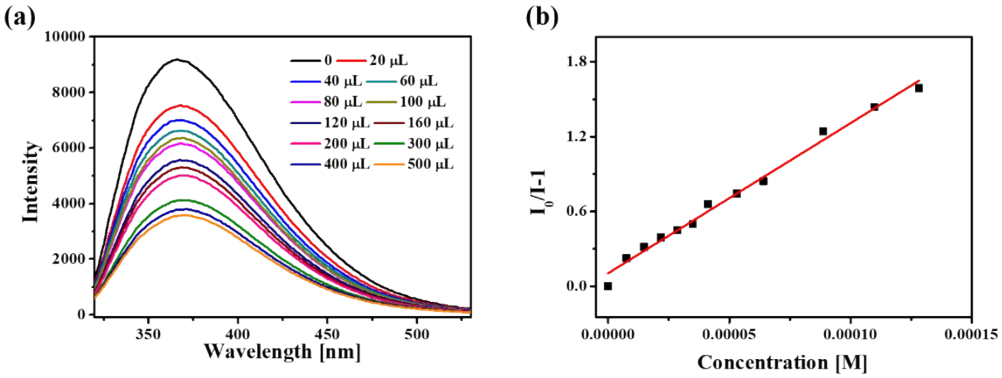

Fig. S24 (a) Effect on the emission spectra of BUT-19 dispersed in water upon the incremental addition of 500 µL (100 ppm) water solution of CAR, (b) Stern-Volmer plot of CAR.

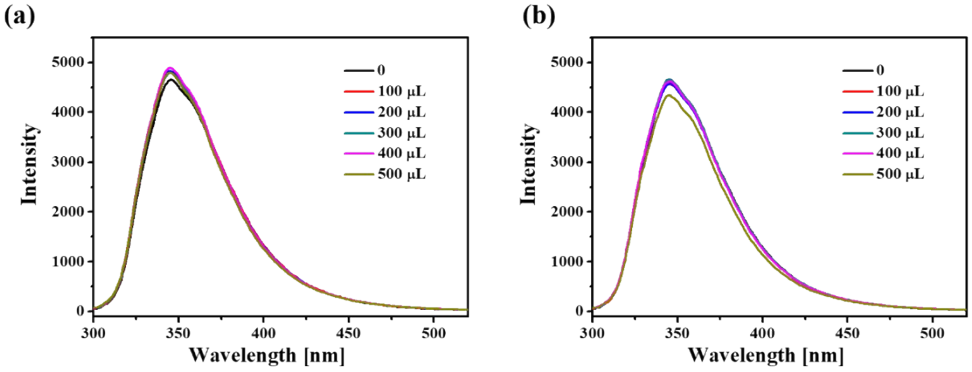

Fig. S25 Effect on the emission spectra of BUT-19 dispersed in water upon the incremental addition of 500 µL (100 ppm) water solution of (a) ERY and (b) THI, respectively.

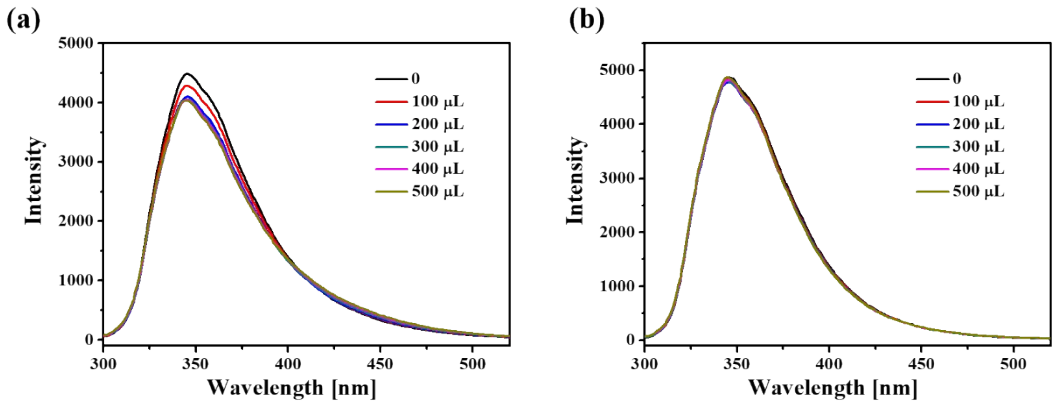

Fig. S26 Effect on the emission spectra of BUT-18 dispersed in water upon the incremental addition of 500 µL (100 ppm) water solution of (a) CYP and (b) PEN, respectively.

Table S1. Summary of K_{sv} of **BUT-18** and **-19** for sensing organic arsenics at RT.

BUT-18	K_{sv} (M^{-1})	**BUT-19**	K_{sv} (M^{-1})
ROX	185467	ROX	229198
NIT	84664	NIT	219267
HAA	4172	HAA	5283
ASA	1976	ASA	14243
CAR	383	CAR	12037

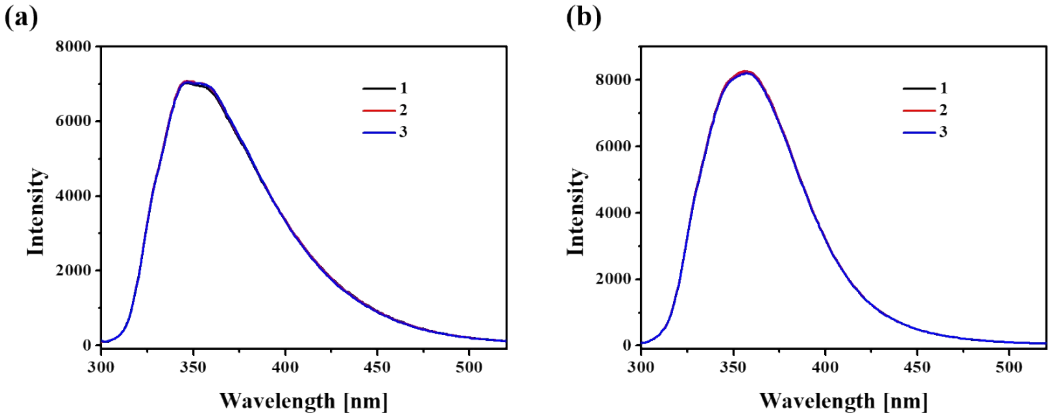

Fig. S27 Three repeated fluorescent measurements of blank solutions of (a) BUT-18 and (b) BUT-19.

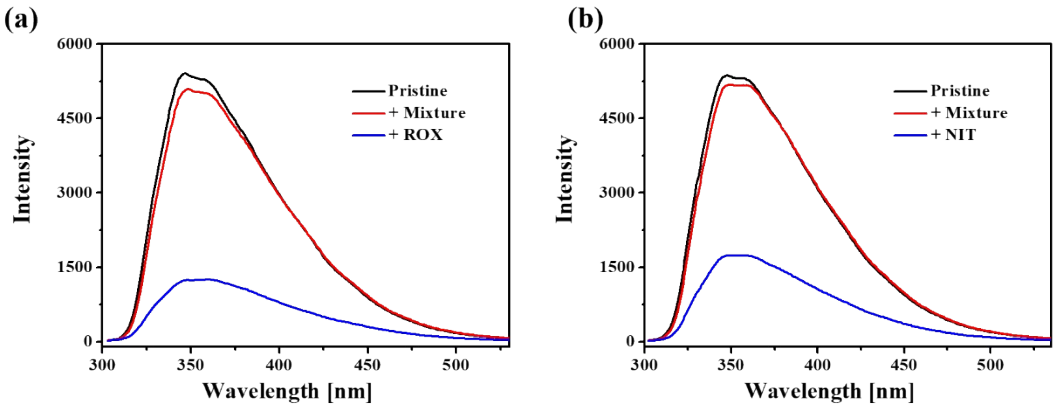

Fig. S28 Fluorescent spectra of BUT-18 upon the addition of (a) ROX and (b) NIT (500 μL, 100 ppm) in the presence of a mixture of 4 drugs (100 ppm for each interferent) in water, monitored at 280 nm.

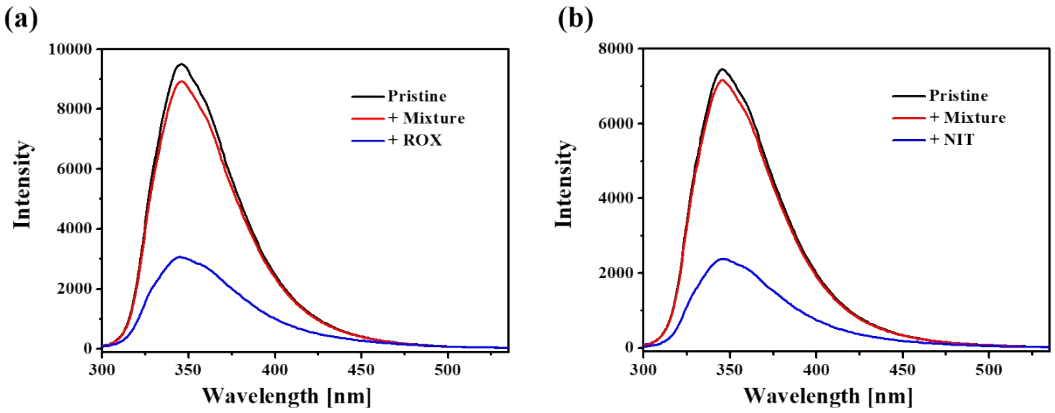

Fig. S29 Fluorescent spectra of BUT-19 upon the addition of (a) ROX and (b) NIT (500 μL, 100 ppm) in the presence of a mixture of 4 drugs (100 ppm for each interferent) in water, monitored at 280 nm.

Table S2. HOMO and LUMO energies calculated for selected anlytes used at B3LYP/6-31G* level.

Analyte	HOMO	LUMO	GAP
ROX	-7.909	-3.140	4.769
NIT	-8.515	-3.518	4.997
HAA	-7.199	-1.370	5.829
ASA	-6.521	-1.127	5.394
CAR	-7.051	-1.692	5.359
CYP	-6.585	-1.316	5.269
ERY	-6.120	-0.907	5.213
PEN	-5.558	-1.777	3.781
THI	-6.206	-2.661	3.545
BUT-18	-6.008	-3.070	2.938
BUT-19	-6.140	-3.130	2.974

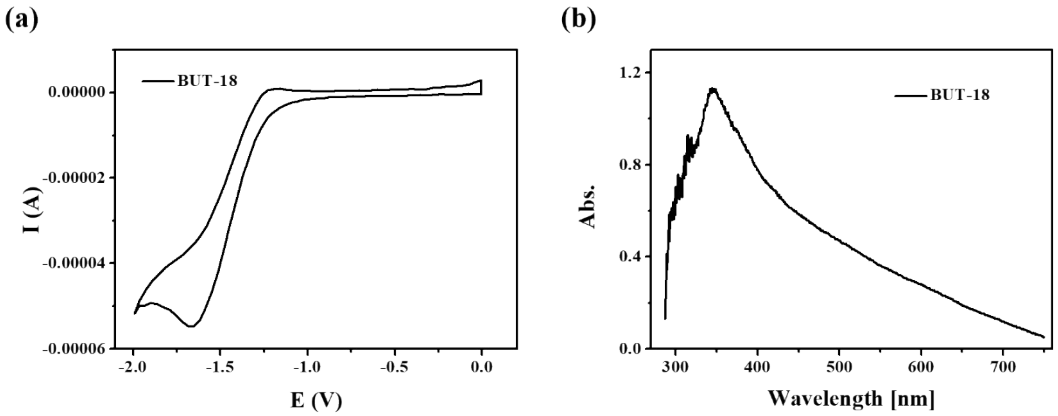

Fig. S30 (a) CV curve of BUT-18 in THF, (b) UV-vis spectrum of BUT-18 in water.

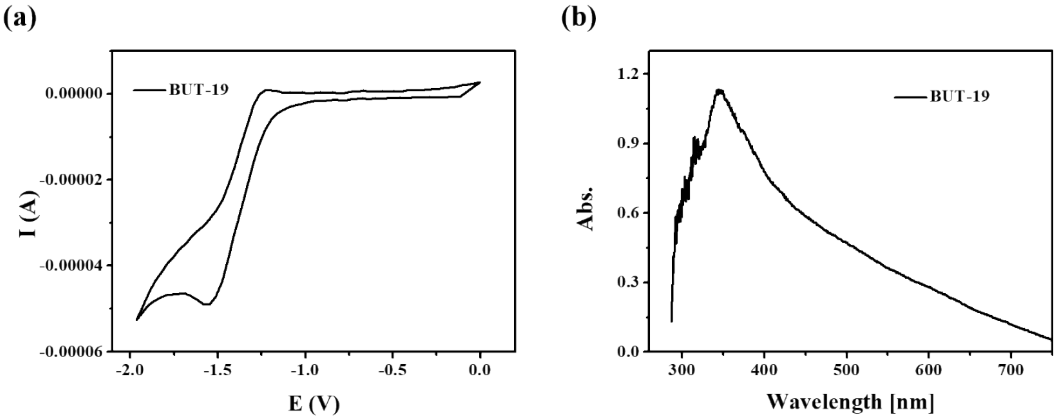

Fig. S31 (a) CV curve of BUT-19 in THF, (b) UV-vis spectrum of BUT-19 in water.

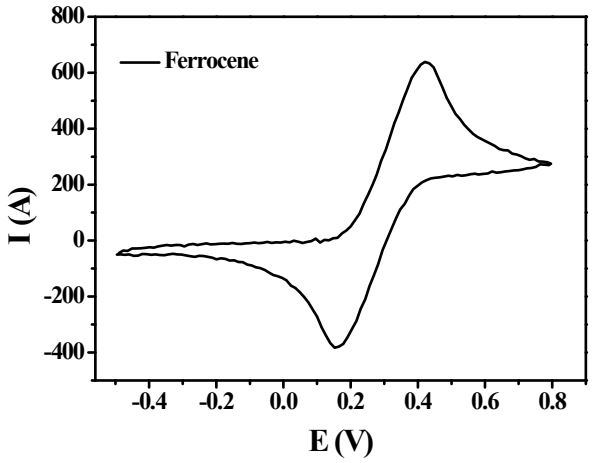

Fig. S32 CV curve of Ferrocene in THF.

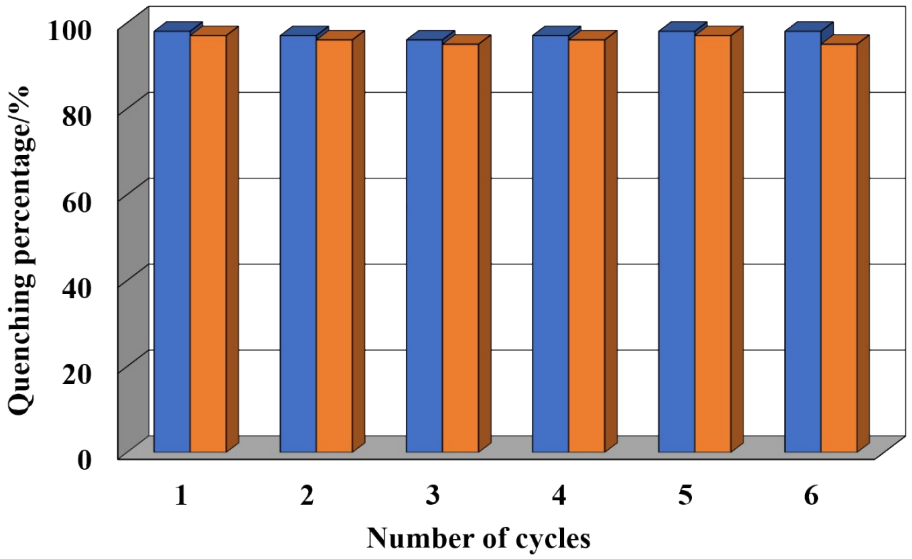

Fig. S33 Reproducibility of the quenching ability of BUT-18 (blue bar) and BUT-19 (orange bar) by ROX.